



Hippocampal subfield transcriptome analysis in schizophrenia psychosis

Jessica Marie Perez¹ · Stefano Berto² · Kelly Gleason¹ · Subroto Ghose¹ · Chunfeng Tan¹ · Tae-Kyung Kim³ · Genevieve Konopka² · Carol A Tamminga¹

Received: 22 July 2019 / Revised: 16 January 2020 / Accepted: 19 February 2020 / Published online: 9 March 2020
© The Author(s), under exclusive licence to Springer Nature Limited 2020

Abstract

We have previously demonstrated functional and molecular changes in hippocampal subfields in individuals with schizophrenia (SZ) psychosis associated with hippocampal excitability. In this study, we use RNA-seq and assess global transcriptome changes in the hippocampal subfields, DG, CA3, and CA1 from individuals with SZ psychosis and controls to elucidate subfield-relevant molecular changes. We also examine changes in gene expression due to antipsychotic medication in the hippocampal subfields from our SZ ON- and OFF-antipsychotic medication cohort. We identify unique subfield-specific molecular profiles in schizophrenia postmortem samples compared with controls, implicating astrocytes in DG, immune mechanisms in CA3, and synaptic scaling in CA1. We show a unique pattern of subfield-specific effects by antipsychotic medication on gene expression levels with scant overlap of genes differentially expressed by SZ disease effect versus medication effect. These hippocampal subfield changes serve to confirm and extend our previous model of SZ and can explain the lack of full efficacy of conventional antipsychotic medication on SZ symptomatology. With future characterization using single-cell studies, the identified distinct molecular profiles of the DG, CA3, and CA1 in SZ psychosis may serve to identify further potential hippocampal-based therapeutic targets.

Introduction

Schizophrenia affects millions of people worldwide with 10% of those diagnosed with schizophrenia eventually committing suicide [1]. Its complex clinical profile is responsible for schizophrenia being a top 10 leading cause of disability in adolescents and young adults [2]. The positive symptoms, which emerge during young adulthood,

include hallucinations, delusions, and thought disorder and are commonly referred to as psychosis. Negative symptoms can include anhedonia and asociality while cognitive symptoms involve deficits in memory, executive function, and attention [3].

Unfortunately, antipsychotics are not curative as they only address the psychotic symptoms. Also, 20–33% of individuals are unresponsive to these treatments [4–6]. In addition, treatment with antipsychotics is accompanied by significant adverse side effects [7], dramatically reducing patient medication compliance [8]. Rational treatment development motivates the elucidation of the molecular mechanisms underlying SZ pathology, which remain largely unknown.

Several studies have implicated the hippocampus in SZ [9–12], and from our data, we have based a model of psychosis in which the hippocampal subfields play distinct roles in SZ pathology [13–15]. We hypothesize that reductions in excitatory afferent stimulation between DG and CA3 are associated with CA3 hyperactivity leading to hippocampal alterations in learning and memory in individuals with schizophrenia. The loss of excitatory activity in DG may contribute to reduced pattern separation. This

Supplementary information The online version of this article (<https://doi.org/10.1038/s41380-020-0696-6>) contains supplementary material, which is available to authorized users.

✉ Jessica Marie Perez
Jessicapere18@gmail.com

- ¹ Division of Translational Neuroscience in Schizophrenia, Department of Psychiatry, University of Texas Southwestern Medical Center, Dallas, TX 75390, USA
- ² Department of Neuroscience, UT Southwestern Medical Center, Dallas, TX 75390, USA
- ³ Department of Life Sciences, Pohang University of Science and Technology, Pohang, Gyeongbuk 37673, Korea

could shift the hippocampus' computational cognition bias from separation to completion and lead to an inability to distinguish novel stimuli and previous associations in memories [16]. This shift could plausibly generate false memories and create vulnerability toward the production of psychotic experiences [13].

Therefore, we sought to determine the contribution of the individual hippocampal subfields in generating the psychosis molecular blueprint our lab has previously shown [13, 14]. Given the complex nature of schizophrenia, we used next-generation sequencing to identify in a global, systematic, and unbiased manner psychosis-mediating molecular candidates, which have not been previously implicated in SZ. The current study is the first to examine the transcriptome of the hippocampal subfields from the same set of individuals with schizophrenia and matched controls, offering a deep examination of gene expression changes in SZ in the hippocampus.

Materials and methods

Human postmortem tissue collection

Human brain tissue was obtained from the University of Texas Southwestern Medical Center (UTSW) Dallas Brain Collection. The UTSW Institutional Review Board approved the collection of human brain tissue. Cases within 24 h of death on average, with schizophrenia or healthy diagnoses, without agonal duress or other brain disorders, were collected with next of kin consent [14, 17]. Diagnoses were advantaged by review of available medical records and an informant interview. Characteristically, four psychiatrists or a minimum of two made independent diagnoses and developed a consensus diagnosis [17]. A high-quality tissue cohort with DG, CA3, and CA1-enriched samples was created from schizophrenia ($N=13$: $N=6$ SZ ON-antipsychotic medication and $N=7$ SZ OFF-antipsychotic medication) and healthy control (HC) cases ($N=13$). "OFF-antipsychotic medication" was confirmed by negative plasma and vitreous antipsychotic drug levels at autopsy, family history of no recent medication use, and/or pharmacy records whenever available [14]. Schizophrenia and HC were matched based on RNA integrity number (RIN), PMI, age, gender, and BMI as closely as possible. Supplementary Table 1 includes demographic information for the samples used in this study.

Hippocampal dissections

Frozen hippocampal tissue was sectioned into 300- μ m sections, alternating with 30- μ m sections. Overall, 30- μ m sections were placed in 4% paraformaldehyde solution

overnight for subsequent Nissl staining to determine DG, CA3, and CA1 orientation of hippocampal subfields for dissection. Hippocampal subfields were isolated as previously described [18], and then used for RNA-seq.

RNA extraction

Total RNA was extracted and purified using a protocol combining Trizol and chloroform extraction, the GeneJET RNA Purification Kit, and a motorized mini-pestle vibrator for tissue homogenization. RNA purity and concentration were assessed on the Nanodrop spectrophotometer and Agilent2100 Bioanalyzer for RIN determination. Average RIN ≥ 5 were selected for sequencing.

Library preparation and sequencing

Total RNA sample preparation and sequencing was performed by the McDermott Sequencing Core at UTSW on a preliminary CA3 cohort ($N=5$ SZ OFF medication and $N=5$ HC cases). The UTSW Genomics and Microarray Core sequenced DG and CA1 samples ($N=13$ SZ and $N=13$ HC) as well as CA3 ($N=8$ SZ and $N=8$ HC). Total RNA was rRNA ribo-depleted, and strand-specific cDNA libraries were synthesized before sequencing on an Illumina HiSeq 2500 sequencer. Stranded, single-end 50 base-pair reads were generated for the preliminary CA3 cohort data. Stranded paired-end 100 base-pair reads were generated for additional cohorts.

RNA-seq mapping, QC and expression quantification

Adapter removal and quality trimming was performed using Trimmomatic [19]. Reads were aligned to the human hg19 reference genome using STAR 2.5.2b [20] with the following parameters: "--outFilterMultimapNmax 10 --alignSJoverhangMin 10 --alignSJDBoverhangMin 1 --outFilterMismatchNmax 3 --twopassMode Basic". Ensemble annotation for hg19 (GRCh37.87) was used to build STAR indexes. For each sample, a BAM file, including mapped and unmapped reads with spanning splice junctions, was produced. Secondary alignment and multi-mapped reads were removed and uniquely mapped reads were retained. Quality control metrics were performed using RSeqQC and the hg19 gene model [21]. Gene level expression was calculated using HTseq 0.9.1 using intersection-strict mode *by gene* [22]. Counts and gene length were calculated based on protein-coding genes from the Ensemble GRCh37.87 annotation file. CPM values were calculated using edgeR [23] and filtered for differential and coexpression analyses using a "by condition" CPM cutoff. A gene is considered expressed if CPM > 0 in all biological replicates in any of the conditions analyzed.

Differential gene expression analysis (DGEA)

Normalized data were assessed for effects from known biological covariates (diagnosis, age, gender), technical covariates related to sample processing (RIN, PMI, batch), and unknown covariates related to surrogate variation (SV). SVs were calculated using the SVA [24] “be” method with 100 iterations. The data were adjusted for technical covariates using a linear model: $lm(\text{gene expression} \sim \text{Age} + \text{Gender} + \text{PMI} + \text{RIN} + \text{SVs})$. Differentially expressed genes (DEGs) were calculated using linear regression: $lm(\text{gene expression} \sim \text{Diagnosis} + \text{Age} + \text{Gender} + \text{PMI} + \text{RIN} + \text{SVs})$. *P* values were adjusted using the Benjamini-Hochberg procedure [25]. DEGs were determined as those with an estimated FDR < 0.05.

Weighted gene coexpression network analysis (WGCNA)

To identify modules of coexpressed genes in the RNA-seq dataset, WGCNA [26] was performed on 78 samples ($N = 26$ DG; $N = 26$ CA3; $N = 26$ CA1). We generated a signed network via the *blockwiseModules* function. Beta was 14 for a high scale-free $r^2 = 0.79$ network. We used *corType = bicor*, *maxBlockSize = 14000*, *mergingThresh = 0.15*, *reassignThreshold = 1e-10*, *deepSplit = 2*, *detectCutHeight = 0.999*, and *minModuleSize = 50*. Modules were determined using the dynamic tree-cutting algorithm. Module visualizations were created using Cytoscape v3.4.0 [27]. GO analysis was performed using ToppGene (<https://toppgene.cchmc.org>).

Gene expression omnibus (GEO) accession information

The National Center for Biotechnology Information GEO accession number for the RNA-seq data reported in this study is GSE138082 (token: mdypgiqgndgdlkb).

Results

Hippocampus subfield characterization

We used RNA-seq to examine DG, CA3, and CA1 between individuals previously diagnosed with SZ and HC to identify differences between hippocampal circuit transcriptional profiles. Principal component analysis showed marked separation of the subfields based on gene expression variance trends (Fig. 1a), suggesting the importance of conducting hippocampal subfield-specific analyses. The results from each subregion are provided below.

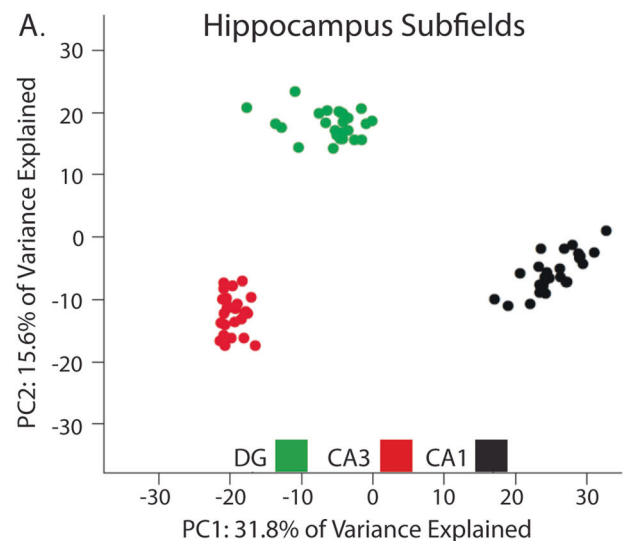
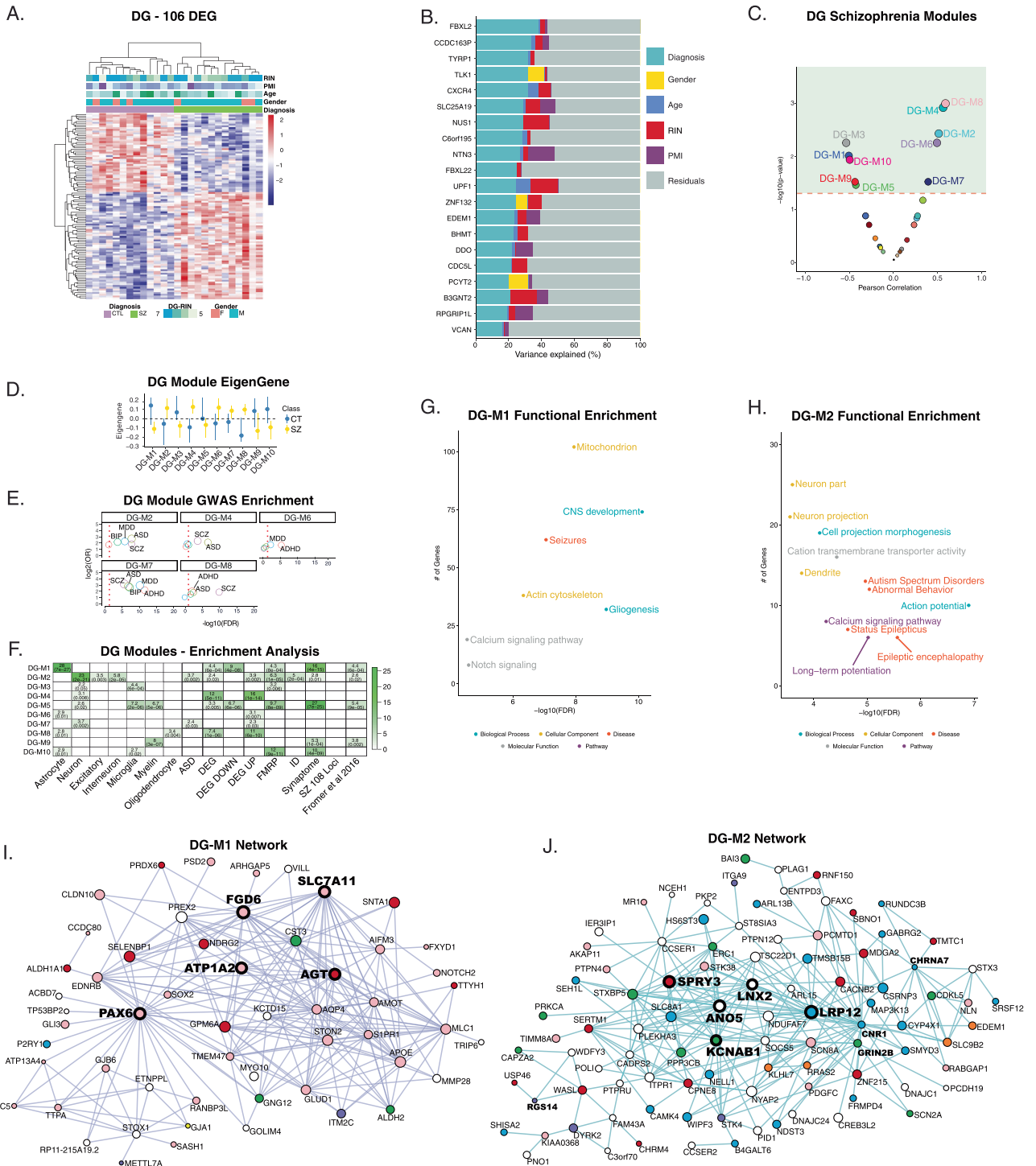


Fig. 1 Principal component analysis (PCA) plot of hippocampal RNA-seq data. **a** PCA characterizing the gene expression variance trends exhibited between hippocampal subfields, DG ($n = 26$), CA3 ($n = 26$), and CA1 ($n = 26$). Each dot represents a sample and each color represents the specific hippocampal subfield.

Dentate gyrus

For each subfield, we assessed differential gene expression using linear model analysis at FDR < 0.05. In DG, we identified 106 DEGs between SZ and HC (Supplementary Table 2) as illustrated by the heatmap (Fig. 2a). Overall, 58% of DEGs were upregulated in the SZ group compared with controls. Because of the heterogeneous nature of human samples, we evaluated percent variance explained (PVE) for the top DEGs. There was no correlation between FDR and PVE by diagnosis (data not shown). Therefore, it was notable that the top DEGs had more variance explained by diagnosis than other known factors combined (Fig. 2b). This result suggests that DEGs chosen for further study have a greater prospect of playing a role in SZ pathology.

DGEA helps evaluate single-gene expression differences across disease states, providing information about plausible gene targets of schizophrenia pathology. However, the polygenic nature of schizophrenia complicates the progression from DEG lists to functionally relevant conclusions about the disorder. SZ polygenicity coincides with disease state being driven by network changes rather than single-gene alterations [28, 29]. Therefore, to continue to formulate evidence toward a comprehensive hypothesis from our RNA-seq dataset, we used WGCNA [26]. This analysis clusters genes into module networks based on related gene coexpression levels, where the most highly coexpressed genes are considered network hubs. Coexpressed genes (i.e., genes with similar expression patterns)



are known to share regulatory mechanisms and converge on similar biological pathways and cellular functions [30]. Therefore, hub genes are suggested to be the main regulators of a module's indicated function. Hub gene association to disease state is a strong implicating factor for target gene identification. Therefore, these networks allow for the identification of higher-order biological relationships

underlying schizophrenia on which single-gene and whole-network alterations converge.

In DG, 30 coexpression modules were identified. Ten modules (DG-M1 through DG-M10) were significantly associated with SZ (Fig. 2c, d, Supplementary Table 3A). To characterize the biological significance of these SZ-associated modules, we conducted enrichment analyses of

◀ **Fig. 2 DGEA and WGCNA characterization of dentate gyrus from individuals with SZ compared with controls.** **a** Heat map of significantly differentially expressed genes identified with LMA between SZ and control samples in DG. Dendrograms depict Pearson correlation clustering of samples. Top bars represent demographics of each sample: RNA integrity number (RIN), postmortem interval (PMI), age, gender, and diagnosis. Corresponding scales of gene expression levels and demographics are shown on the right and bottom, respectively. Blue and red color intensities designate downregulation and upregulation, respectively. **b** Bar graphs depicting percent variance explained by each factor after correction for all other factors, including diagnosis, gender, age, RIN, and PMI for several top significantly DEG in DG. **c** Pearson correlation analysis of WGCNA modules to assess module correlation with SZ diagnosis. Out of 30 modules, ten modules above the dashed red line are significantly correlated with SZ. **d** Module eigengenes of the ten modules significantly positively or negatively associated with schizophrenia. **e** DG modules enriched for genes with genetic risk variants associated with SZ, autism spectrum disorder (ASD), major depressive disorder (MDD), bipolar disorder (BIP), and/or attention deficit hyperactivity disorder (ADHD) using publicly available genome-wide association studies (GWAS) from the Psychiatric Genomics Consortium 2 (PGC2). Significant enrichment is indicated by localization to the right of the red-dashed line. **f** Cell-type and gene set enrichment analysis of DG modules significantly associated with SZ. ASD autism spectrum disorder, DEG differentially expressed genes, DEG DOWN downregulated differentially expressed genes, DEG UP upregulated differentially expressed genes, FMRP fragile X mental retardation protein, ID intellectual disability, synaptome synaptome database, SZ 108 Loci [34]. **g, h** Gene ontology enrichment analysis of SZ-associated DG-M1 and M2 modules. **i, j** Top WGCNA connections of SZ-associated DG-M1 and M2 modules. Node size dimension has a direct relationship with the number of gene coexpression connections. (Red—gene identified by Fromer et al., 2016 and/or Schizophrenia Working Group of the Psychiatric Genomics Consortium, 2014; Green—synaptic genes identified by synaptomeDB; Blue—neuronal genes; Orange—differentially expressed genes; Pink—astrocytic genes; Purple—microglial genes).

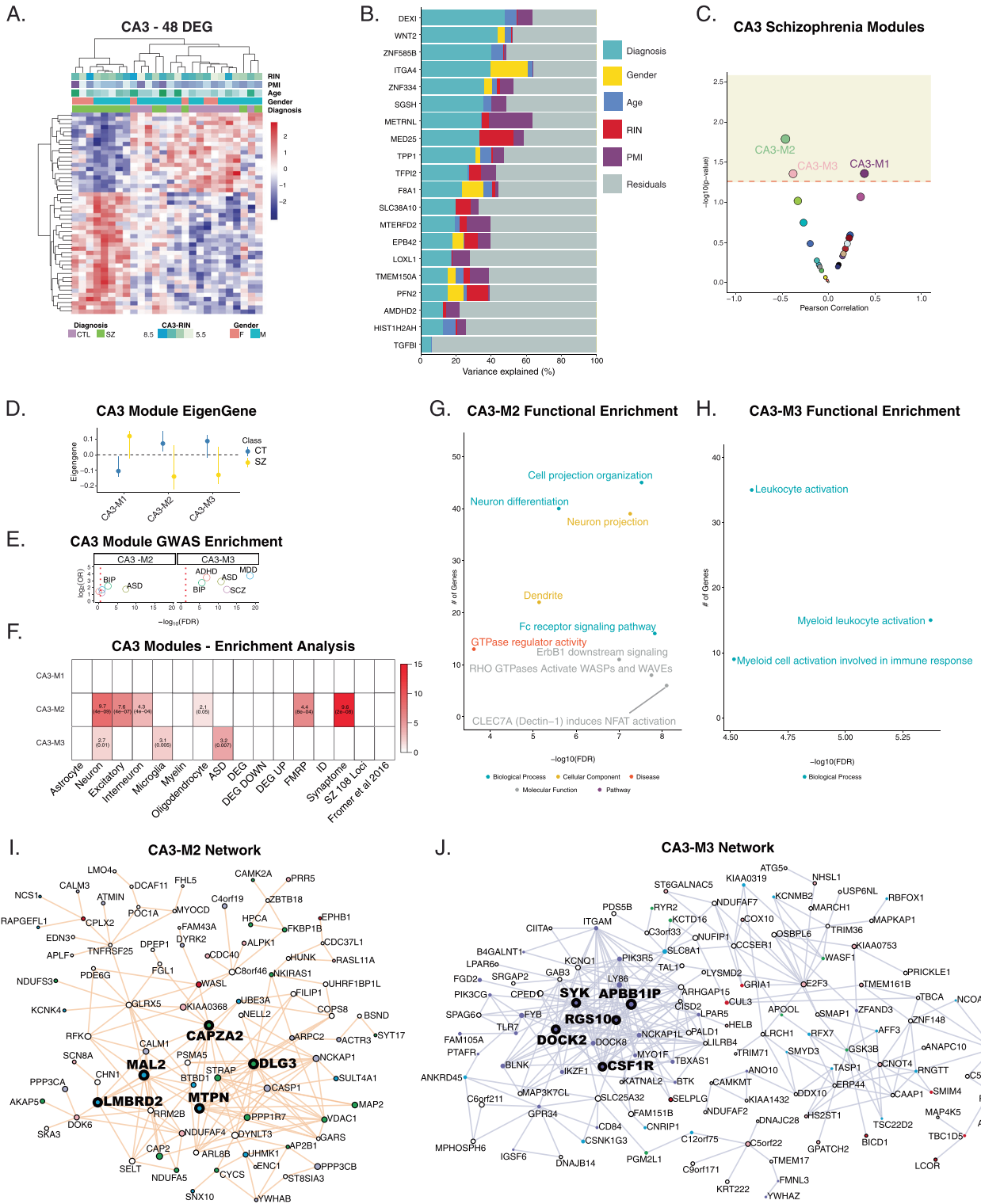
psychiatric disorder common variant genes, cell-type associated genes, and gene ontologies. DG-M2, DG-M4, DG-M7, and DG-M8 were enriched for SZ single nucleotide polymorphism (SNP)-associated genes (Fig. 2e) from the Psychiatric Genomics Consortium 2. DG-M1 was enriched in DEGs and synaptic genes as well as in genes previously identified as differentially expressed in the DLPFC of SZ and HC [31] and astrocytic cell-type genes (Fig. 2f). This links currently identified DEGs and previously identified [31–33] molecular alterations to new astrocytic alterations in the hippocampus. In addition, DG-M2 was enriched for inhibitory and excitatory interneurons, indicating that activity and/or inhibitory cellular function could be compromised as previously suggested by our psychosis model.

Lastly, we looked at functional enrichment analysis in combination with network visualization to characterize a functional role for these SZ-associated modules in psychosis pathology. In DG-M1, gene ontology (GO) analysis showed enrichment for CNS development, gliogenesis, actin cytoskeleton, and calcium signaling pathway (Fig. 2g).

Of these categories, CNS development and gliogenesis were significantly enriched for genes associated with SZ ($p = 0.0486$) from the largest GWAS SZ study to date [34] and for module hub genes ($p = 0.0202$), respectively, implicating this modules' relevance and role in SZ pathology (Fig. 2i). DG-M2 was significantly enriched for GO terms, including ion channel activity, action potential, learning and memory, dendritic spine, and so forth (Fig. 2h). In addition, not only were the ion channel activity and action potential categories enriched with genes from the 108 loci associated with SZ [34] ($p = 0.0234$ and $p = 0.001$, respectively), but the ion channel activity category was also enriched for hub genes ($p = 0.0274$). These two categories comprise genes like *GRIN2B*, *GRIA1*, *CHRNA7*, and *CNRI* (Fig. 2j), genes consistently implicated in SZ pathology in hippocampus [32, 35–37].

Hippocampal CA3

DGEA was conducted in CA3, taking biological, unknown, and technical covariates including batch effects into account, to detect plausible SZ psychosis gene targets. In CA3, we identified 48 DEGs between SZ and HC (Supplementary Table 4) as illustrated by the heatmap in Fig. 3a. Overall, 60% of genes were upregulated in the SZ group compared with HC. Importantly, as in DG, the top DEGs in CA3 had more variance explained by diagnosis than other known factors combined (Fig. 3b). Using WGCNA, 24 modules were generated in CA3, including three significantly associated with SZ (Fig. 3c, d), CA3-M1, CA3-M2, and CA3-M3 (Supplementary Table 3B). The CA3-M2 module was enriched for FMRP and synaptic, oligodendrocyte. In addition, this module was significantly enriched in excitatory neuronal genes (Fig. 3f), revealing a signature of excitatory neurons being affected in CA3 in schizophrenia and corroborating our psychosis model, which implicates hyperactivity in CA3. CA3-M3, the only module enriched in SZ-associated SNP genes (Fig. 3e), was enriched for autism, microglia, and neuronal genes (Fig. 3f). The CA3-M2 module, which consisted of mostly neuronal hub genes (Fig. 3i), was significantly enriched for GO terms including neuron projection, neuron differentiation, and dendrite, as well as pathways involved in the neuroimmune system [38–41] and cell survival and proliferation [42] (Fig. 3g). The CA3-M3 module was enriched in genes from three categories, which all involved the immune system (Fig. 3h). Relevantly, the leukocyte activation category was significantly enriched for hub genes such as *DOCK2*, *SYK*, *APBB1IP* ($p = 0.0051$) (Fig. 3j). The enrichment of genes involved in the neuroimmune system in these CA3 modules is consistent with previous studies showing abnormalities in immune function in schizophrenia [43–48].



Hippocampal CA1

In CA1, we identified 121 DEGs between SZ and HC (Supplementary Table 5) as illustrated in Fig. 4a. Overall,

43% of genes were upregulated in the SZ group. As in DG and CA3, the top DEGs in CA1 had more variance explained by diagnosis than other factors combined (Fig. 4b). Twenty-eight modules were generated in CA1

◀ **Fig. 3 DGEA and WGCNA characterization of CA3 from individuals with SZ compared with controls.** **a** Heat map of significantly differentially expressed genes in CA3 between SZ and control samples. Dendrograms depict Pearson correlation clustering of samples. Top bars represent demographics of each sample: RNA integrity number (RIN), postmortem interval (PMI), age, gender, and diagnosis. Corresponding scales of gene expression levels and demographics are shown on the right and bottom, respectively. Blue and red color intensities designate downregulation and upregulation, respectively. **b** Bar graphs depicting percent variance explained by each factor after correction for all other factors, including diagnosis, gender, age, RIN, and PMI for several top significantly DEG in CA3. **c** Pearson correlation analysis of WGCNA modules to assess correlation with SZ diagnosis. Out of 24 modules, three modules above the dashed red line are significantly correlated with SZ. **d** Module eigengenes of the three modules significantly positively or negatively associated with schizophrenia. **e** CA3 modules enriched for genes with genetic risk variants associated with SZ, ASD, MDD, bipolar disorder, and/or ADHD using publicly available GWAS from the Psychiatric Genomics Consortium 2. Significant enrichment is indicated by localization to the right of the red-dashed line. **f** Cell-type and gene set enrichment analysis of CA3 modules significantly associated with SZ. ASD autism spectrum disorder, DEG differentially expressed genes, DEG DOWN downregulated differentially expressed genes, DEG UP upregulated differentially expressed genes, FMRP fragile X mental retardation protein, ID intellectual disability, synaptome synaptome database, SZ 108 Loci [34]. **g, h** Gene ontology enrichment analysis of SZ-associated CA3-M2 and M3 modules. **i, j** Top WGCNA connections of SZ-associated CA3-M2 and M3 modules. Node size dimension has a direct relationship with the number of gene coexpression connections. (Red—gene identified by Fromer et al., 2016 and/or Schizophrenia Working Group of the Psychiatric Genomics Consortium, 2014; Green—synaptic genes identified by synaptomeDB; Blue—neuronal genes; Orange—differentially expressed genes; Pink—astrocytic genes; Purple—microglial genes and genes from immune system GO category).

with six significantly associated with SZ (Fig. 4c, d), CA1-M1 through CA1-M6 (Supplementary Table 3C). CA1 had three modules, CA1-M2, CA1-M3, CA1-M4, enriched for genes with SZ-associated SNPs (Fig. 4e). CA1-M3 was enriched for autism and synaptic genes and downregulated DEGs as well as astrocytic, oligodendrocyte, and excitatory neuronal genes (Fig. 4f). In addition, CA1-M3 was enriched in genes from GO categories like ion channel activity, postsynaptic membrane, and postsynaptic density (PSD) (Fig. 4g), which follows the pattern of activity-related alterations previously seen in DG and CA3. The PSD category was enriched for genes from the 108 loci associated with SZ [34] ($p = 0.0352$), including genes previously associated with SZ like *DABI*, *GRIA2*, *GRIN2A*, *GRM1*, and *BDNF* (Fig. 4h). It was also enriched in genes involved in the glutamatergic synapse pathway and the disease category, schizophrenia (Fig. 4g). Together, these results imply that the genes coexpressed in these modules are particularly important in governing SZ pathology and that module functions associated with SZ are distinct by hippocampal subfield.

Antipsychotic medication effect

Antipsychotic medications alter gene expression levels in animals and individuals with schizophrenia [49–51]. To exclude a potential antipsychotic medication effect on gene expression levels, we examined differential gene expression in ON- and OFF-antipsychotic medication SZ samples in DG, CA3, and CA1. Eighty genes were differentially expressed in DG, 351 in CA3, and 188 in CA1 between the ON and OFF groups (Fig. 5a) as illustrated by the heatmaps (Fig. 5b–d). Overall, 49%, 40%, and 49% of genes in DG, CA3, and CA1, respectively, were upregulated in the ON group. The amount of variance explained by antipsychotic medication (Fig. 5e–g) compared with diagnosis (Figs. 2b, 3b and 4b) was considerably different. The highest variance explained by medication for top DEGs in DG was 65% versus 38% by diagnosis. In CA1, top DEGs had 72% variance explained by medication versus 50% by diagnosis. While there were ~300 more DEGs in the CA3 medication cohort compared with the SZ cohort, the amount of variance explained by medication was only 37% compared with 48% by diagnosis. Together, these results propose a more potent effect of antipsychotic medication to alter gene expression than diagnosis and a subfield-specific medication effect. The number of DEGs due to diagnosis had minimal overlap with DEGs due to medication effect (Fig. 5h–j). *SMIM17* and *CTHRC1* were differentially expressed in DG and CA3, respectively, in the SZ and medication cohorts. Both genes were increased in the SZ cohort, but decreased in the ON-medication cohort. The results generated by the ON- versus OFF groups, while limited in sample size, illustrate the complexity bound to research of severe mental illness. While future verification of this experiment in a larger sample size is necessary, these results may indicate plausible medication targets.

Discussion

This study examined the DG, CA3, and CA1 transcriptomes from the same cohort of postmortem samples in individuals with schizophrenia and matched controls. This eliminated the caveat that differences in gene expression by subfield could be due to disparate subfield populations rather than biologically relevant subfield changes. Indeed, our results support our hypothesis and emerging idea that hippocampal functionality differs by subfield. The hippocampus deserves subfield-specific experimental scrutiny to characterize the hippocampus and disorders like schizophrenia properly.

One caveat that accompanies the examination of human tissue is the inability to control all environmental variables. Consequently, the field typically assembles cohorts by

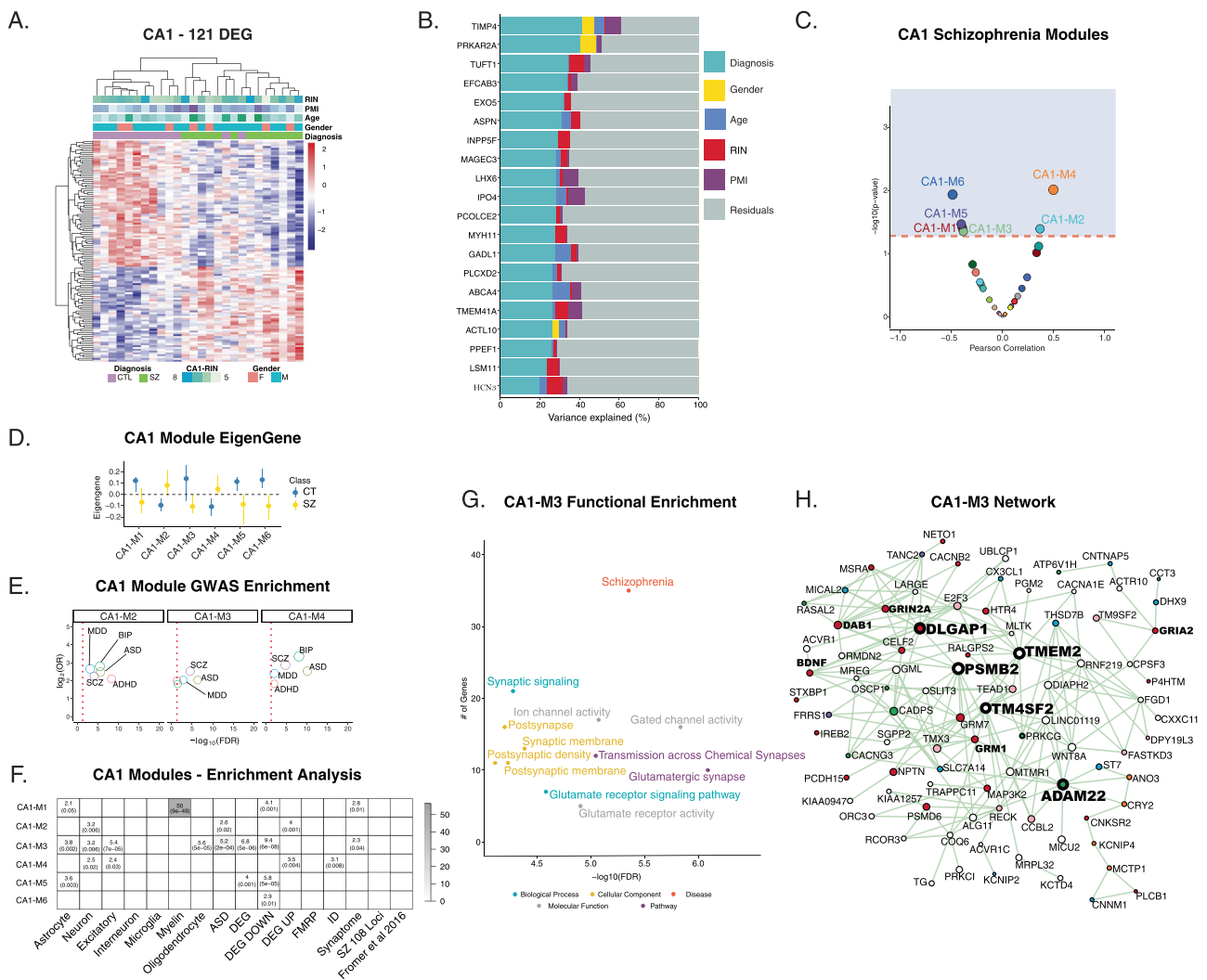


Fig. 4 DGEA and WGCNA characterization of CA1 from individuals with SZ compared to controls. **a** Heat map of significantly differentially expressed genes in CA1 between SZ and control samples. Dendrograms depict Pearson correlation clustering of samples. Top bars represent demographics of each sample: RNA integrity number (RIN), postmortem interval (PMI), age, gender, and diagnosis. Corresponding scales of gene expression levels and demographics are shown on the right and bottom, respectively. Blue and red color intensities designate downregulation and upregulation, respectively. **b** Bar graphs depicting percent variance explained by each factor after correction for all other factors, including diagnosis, gender, age, RIN, and PMI for several top significantly DEG in CA1. **c** Pearson correlation analysis of WGCNA modules to assess correlation with SZ diagnosis. Out of 28 modules, six modules above the dashed red line are significantly correlated with SZ. **d** Module eigengenes of the six modules significantly positively or negatively associated with schizophrenia. **e** CA1 modules enriched for genes with genetic risk variants associated with SZ, ASD, MDD, bipolar disorder, and/or ADHD

using publicly available GWAS from the Psychiatric Genomics Consortium 2. Significant enrichment is indicated by localization to the right of the red-dashed line. **f** Cell-type and gene set enrichment analysis of CA1 modules significantly associated with SZ. ASD autism spectrum disorder, DEG differentially expressed genes, DEG DOWN downregulated differentially expressed genes, DEG UP upregulated differentially expressed genes, FMRP fragile X mental retardation protein, ID intellectual disability, synaptome synaptome database, SZ 108 Loci [34]. **g** Gene ontology enrichment analysis of SZ-associated CA1-M3 module. **i, j** Top WGCNA connections of SZ-associated CA1-M3 module. Node size dimension has a direct relationship with the number of gene coexpression connections. (Red—gene identified by Fromer et al., 2016 and/or Schizophrenia Working Group of the Psychiatric Genomics Consortium, 2014; Green—synaptic genes identified by synaptomeDB; Blue—neuronal genes; Orange—differentially expressed genes; Pink—astrocytic genes; Purple—microglial genes).

matching experimental and control samples by variables like age, gender, PMI, and RIN [17]. However, this practice does not guarantee that these variables will not affect the results of a gene expression study, possibly obscuring the physiological relevance of identified gene expression

changes. In fact, experimenters have declared it unfeasible to identify relevant gene expression changes unless thousands of samples are analyzed [31]. It is important to note that this study defined relevant gene changes as those in genes implicated in SCZ-associated eQTL and conjectured

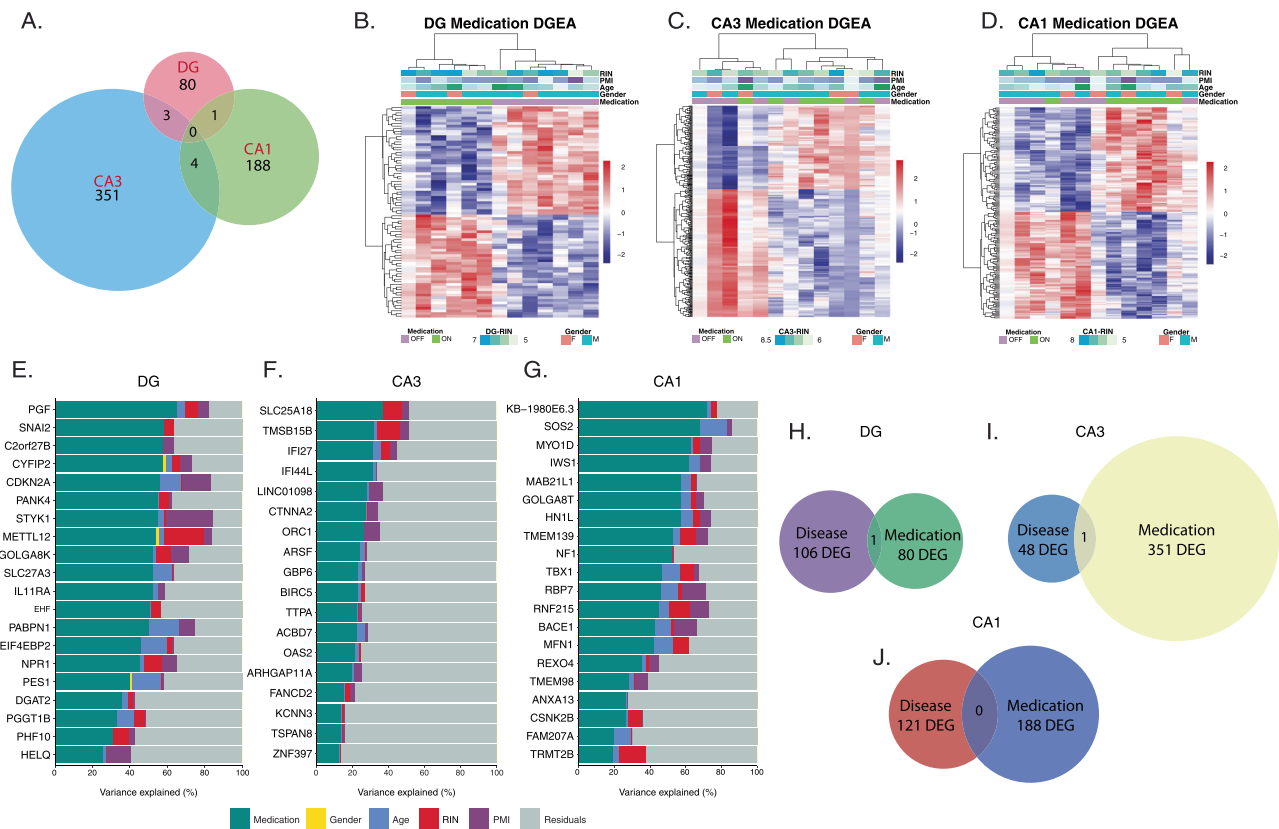


Fig. 5 Gene expression changes in hippocampal subfields, DG, CA3, and CA1, in individuals with SZ either ON- or OFF-antipsychotic medication. **a** Venn diagram depicting the overlap of genes differentially expressed between individuals with SZ ON- and SZ OFF-antipsychotic medication in hippocampal subfields, DG, CA3, and CA1. Differential expression was assessed with linear model analysis (LMA), at a false-discover rate (FDR) <0.05. Heat maps of significantly differentially expressed genes between SZ ON- and SZ OFF-antipsychotic medication in **b** DG, **c** CA3, and **d** CA1. Dendograms depict Pearson correlation clustering of samples. Top bars represent demographics of each sample: RNA integrity number (RIN),

postmortem interval (PMI), age, gender, and antipsychotic medication. Corresponding scales of gene expression levels and demographics are shown on the right. Blue and red color intensities designate down-regulation and up-regulation, respectively. Bar graphs depicting percent variance explained in **e** DG, **f** CA3, and **g** CA1 by each factor after correction for all other factors, including antipsychotic medication, gender, age, RIN, and PMI for gene transcriptome signatures from several top significantly DEGs. Venn diagrams depicting the overlap of genes differentially expressed (DE) due to disease effect versus genes DE due to antipsychotic medication effect in hippocampal subfields (**h**) DG, **i** CA3, **j** and CA1.

that genome-wide studies with smaller sample sizes would have larger variability estimates, translating into false positives with large differential expression estimates. Although our study has a smaller sample size, it produced few differential estimates exceeding twofold, which is inconsistent with the pattern hypothesized and instead emulates the pattern seen when *N* is raised to 250. These results support our hypothesis that the hippocampal subfields individually play a more pivotal role in SZ psychosis than other heterogeneous tissues like DLPFC or whole hippocampus, brain regions typically probed when investigating schizophrenia. Notably, our analysis of PVE allowed us to choose gene targets for future study more effectively by preferring genes with a majority of PVE by diagnosis and minimal PVE by other confounding variables.

To select in a hypothesis-generating approach novel target genes that may account for the complexity of SZ, we

converged analytical techniques. Along with DGEA, we applied WGCNA to study gene network alterations, which may be critical to SZ pathology. Our study indicated that modules associated with schizophrenia were functionally unique across hippocampal subfields. Target genes were chosen based on PVE by diagnosis, lack of PVE by other variables, significant association with diagnosis in multiple analyses (DGEA, WGCNA, GO), and establishment in the literature.

DG SZ-associated modules showed a distinct astrocytic profile, including hub genes like *PAX6*. In the adult hippocampus, neurogenesis is thought to occur in the subgranular zone (SGZ) of DG [52]. The SGZ contains type-1 stem cells, which share similar characteristics to astrocytes including GFAP expression. *PAX6* is expressed in both SGZ type-1 stem cells [53] and hippocampal astrocytes [54]. In a study examining the process of cell-population

balance between neurogenesis and gliogenesis in the adult hippocampus, increased *PAX6* drove maturation of newly born neurons [55]. Conversely, reductions in *PAX6* reduced the progenitor cell pool necessary for neurogenesis in DG [53], inhibited astrocyte maturation and increased Akt activity [54]. Not only has the Akt pathway been genetically linked to schizophrenia [56], but antipsychotic medications have also been repeatedly shown to increase activated Akt levels [57, 58]. However, it is still unclear whether this antipsychotic-mediated increase improves psychosis symptomatology. Because adult-born granule cells play a critical role in the DG's ability to execute pattern separation [59–61], which our psychosis model hypothesizes may be altered in schizophrenia psychosis, it will be interesting to investigate the role that preservation of cell-population balance or lack thereof plays in SZ pathology.

CA3 modules associated with SZ suggested an immune system profile with hub genes like *DOCK2*. A subclass of nonsteroidal anti-inflammatory drugs (NSAIDs), which mediate anti-inflammatory effects through cyclooxygenase-2 (COX-2) inhibition, have been shown to have a positive effect on total symptom severity as measured by the Positive and Negative Syndrome Scale (PANSS) score in schizophrenia [62] or a positive effect on the positive symptom subscore of the PANSS [63]. Unfortunately, human clinical trials using COX-2 inhibitor NSAIDs have resulted in significant COX-2 inhibition toxicity side effects [64–66]. The field has looked for alternative therapeutic targets, one of which is our SZ-associated gene, *DOCK2*, which was shown to be microglia-specific and regulate innate immunity independent of COX-2 [67]. Links between neuronal activity and microglia processes have been demonstrated in the hippocampus [68] and cortex [69], suggesting that microglial cells may provide a feedback mechanism for neuronal activity regulation [70]. In fact, microglia depletion in mice showed decreased GluN2B expression, without affecting neuronal or synaptic density in the cortex and hippocampus, and GluN2A-driven cortical current responses [71], which may suggest a microglial role in the neurodevelopmental switch from mostly GluN2B-containing NMDARs to mostly GluN2A-containing NMDARs. Because our psychosis model of hyperactivity in CA3 is based on our previous studies that showed increases in GluN2B-containing receptors in CA3 tissue of SZ postmortem tissue compared with HCs [14, 32], our current data could suggest that there is a neurodevelopmental deficit inhibiting the activity-dependent transition in NMDAR composition. Indeed, cell-type enrichment analysis revealed a robust signature of excitatory neurons being affected in CA3 in SZ.

CA1 SZ-associated modules showed an activity-related profile with hub genes like *DLGAP1*. *DLGAP1* encodes a

protein mainly localized to dendrites and the postsynapse of excitatory synapses [72] which contributes to synaptic scaling mediated by Ca^{2+} influx through the NMDAR [73]. Overexpression of *DLGAP1* in hippocampal neurons eliminated homeostatic activity-dependent regulation of AMPAR surface expression [73]. Our previous examinations of CA1 did not find changes in markers of activity [14]. However, our current results suggest that markers of increased activity that we previously identified in CA3 [14] may project downstream to CA1, but in a subtle and attenuated manner, highlighting the importance of global gene expression analyses for intricate disorders like schizophrenia psychosis. Moreover, upregulated DEGs enriched for inhibitory genes and downregulated DEGs enriched for excitatory genes in CA1 suggest compensatory changes to up-field hyperactivity from CA3. A summary of all identified genes of interest from DG, CA3, and CA1 can be found in Supplementary Fig. 1.

This study is the first to capture the globally distinct nature of the hippocampal subfields and their unique involvement in SZ pathophysiology. Previous RNA-seq studies in postmortem schizophrenia hippocampus tissue analyzed DG granule cells [74] or whole hippocampus [48]. Even the latest RNA-seq study published earlier this year analyzed the hippocampus in schizophrenia using whole hippocampus samples to contrast hippocampus and DLPFC [75]. For a complete review of the literature on molecular alterations in the medial temporal lobe in schizophrenia, see Bobilev et al. [76]. In contrast, our study specifically focused on hippocampal subfield analyzes. Our study highlights the value in analyzing subfields distinctly as well as the critical contribution that specific cell populations like astrocytes and microglia may be playing in psychosis. Therefore, now that we have demonstrated distinct transcriptomic profiles in SZ by subfield, it will be further informative to carry out single-cell expression studies.

Another caveat that commonly accompanies postmortem schizophrenia studies is antipsychotic medication and its effect on gene expression levels. This makes it difficult to decipher medication versus disease effect. We address this limitation by analyzing ON- versus OFF-medication SZ samples. Intriguingly, our results indicated a subfield-specific effect of medication on gene expression levels. In addition, we saw scant overlap in DEGs by disease versus medication, which may suggest a reason for the ineffective nature of antipsychotics in treating schizophrenia symptomatology.

In summary, our study showed distinctive hippocampal subfield molecular identities for SZ psychosis samples and ON samples. This is consistent with our model of SZ psychosis. Our results suggest cell functions, which are disordered by subfield as well as novel molecular entities we did not previously consider.

Code availability

Custom R codes and data to support the data analysis are available at https://github.com/konopkalab/Hippo_Subfields.

Acknowledgements We wish to thank the next of kin of the brain tissue donors who made this study possible, the Dallas County Medical Examiners' Office, UT Southwestern Transplant Service and Willed Body Program for assistance with procurement of tissue. This project could not have been performed without the support and generosity of Dr Kenneth Altshuler. This project was performed with funding from the Stanton Sharp Distinguished Chair Endowment and T32 MH076690 Basic Science Training Program in Neurobiology of Mental Illness.

Compliance with ethical standards

Conflict of interest The authors declare that they have no conflict of interest.

Publisher's note Springer Nature remains neutral with regard to jurisdictional claims in published maps and institutional affiliations.

References

- Andreasen B. Introductory textbook of psychiatry. 4th ed. American Psychiatric, Washington, DC, 2006.
- Vos T, Allen C, Arora M, Barber RM, Bhutta ZA, Brown A, et al. Global, regional, and national incidence, prevalence, and years lived with disability for 310 diseases and injuries, 1990–2015: a systematic analysis for the Global Burden of Disease Study 2015. *Lancet*. 2016;388:1545–602.
- Strauss JS, Carpenter WT, Bartko JJ. The diagnosis and understanding of schizophrenia. Part III. Speculations on the processes that underlie schizophrenic symptoms and signs. *Schizophr Bull*. 1974;11:61–9.
- Davis JM, Casper R. Antipsychotic drugs. *Drugs*. 1977;14:260–82.
- Stone JM, Raffin M, Morrison P, Mcguire PK. The biological basis of antipsychotic response in schizophrenia. *J Psychopharmacol*. 2010;24:953–64.
- Conley RR, Kelly DL. Management of treatment resistance in schizophrenia. *Biol Psychiatry*. 2001;50:898–911.
- Uçok A, Gaebel W. Side effects of atypical antipsychotics: a brief overview. *World Psychiatry*. 2008;7:58–62.
- Valenstein M, Blow FC, Copeland LA, McCarthy JF, Zeber JE, Gillon L, et al. Poor antipsychotic adherence among patients with schizophrenia: medication and patient factors. *Schizophr Bull*. 2004;30:255–64.
- Heckers S, Stone D, Walsh J, Shick J, Koul P, Benes FM. Differential hippocampal expression of glutamic acid decarboxylase 65 and 67 messenger RNA in bipolar disorder and schizophrenia. *Arch Gen Psychiatry*. 2002;59:521–29.
- Sinkus ML, Adams CE, Logel J, Freedman R, Leonard S. Expression of immune genes on chromosome 6p21.3–22.1 in schizophrenia. *Brain Behav Immun*. 2013;32:51–62.
- Benes FM. Evidence for altered trisynaptic circuitry in schizophrenic hippocampus. In: *Biological psychiatry*. Biological Psychiatry, 1999;46:589–99.
- Ruzicka W, Subburaju S, Benes FM. Circuit- and diagnosis-specific DNA methylation changes at gamma-aminobutyric acid-related genes in postmortem human hippocampus in schizophrenia and bipolar disorder. *JAMA Psychiatry*. 2015;72:541–51.
- Tamminga CA, Stan AD, Wagner AD. The hippocampal formation in schizophrenia. *Am J Psychiatry*. 2010;167:1178–93.
- Li W, Ghose S, Gleason K, Begovic A, Perez J, Bartko J, et al. Synaptic proteins in schizophrenia hippocampus indicate increased neuronal activity in CA3. *Am J Psychiatry*. 2015;172:373–82.
- Segev A, Yanagi M, Scott D, Southcott SA, Lister JM, Tan C, et al. Reduced GluN1 in mouse dentate gyrus is associated with CA3 hyperactivity and psychosis-like behaviors. *Mol Psychiatry*. 2018. <https://doi.org/10.1038/s41380-018-0124-3>.
- Yassa MA, Stark CE. Pattern separation in the hippocampus. *Trends Neurosci*. 2011;34:515–25.
- Stan AD, Ghose S, Gao XM, Roberts RC, Lewis-Amezquita K, Hatanpaa KJ, et al. Human postmortem tissue: what quality markers matter? *Brain Res*. 2006;1123:1–11.
- Ghose S, Winter MK, McCarron KE, Tamminga CA, Enna SJ. The GABA β receptor as a target for antidepressant drug action. *Br J Pharmacol*. 2011;162:1–17.
- Bolger AM, Lohse M, Usadel B. Trimmomatic: a flexible trimmer for Illumina sequence data. *Bioinformatics*. 2014;30:2114–20.
- Dobin A, Davis CA, Schlesinger F, Drenkow J, Zaleski C, Jha S, et al. STAR: ultrafast universal RNA-seq aligner. *Bioinformatics*. 2013;29:15–21.
- Wang L, Wang S, Li W. RSeQC: quality control of RNA-seq experiments. *Bioinformatics*. 2012;28:2184–5.
- Anders S, Pyl PT, Huber W. HTSeq-A python framework to work with high-throughput sequencing data. *Bioinformatics*. 2015;31:166–9.
- Robinson MD, McCarthy DJ, Smyth GK. edgeR: a bioconductor package for differential expression analysis of digital gene expression data. *Bioinformatics*. 2010;26:139–40.
- Leek JT, Johnson WE, Parker HS, Jaffe AE, Storey JD. The sva package for removing batch effects and other unwanted variation in high-throughput experiments. *Bioinformatics*. 2012;28:882–3.
- Benjamini Y, Hochberg Y. Controlling the false discovery rate: a practical and powerful approach to multiple testing. *J R Stat Soc*. 1995;57:289–300.
- Zhang B, Horvath S. A general framework for weighted gene co-expression network analysis. *Stat Appl Genet Mol Biol*. 2005;4.
- Shannon P, Markiel A, Ozier O, Baliga NS, Wang JT, Ramage D, et al. Cytoscape: a software environment for integrated models of biomolecular interaction networks. *Genome Res*. 2003;13:2498–504.
- Schadt EE. Molecular networks as sensors and drivers of common human diseases. *Nature*. 2009;461:218–23.
- Gaiteri C, Ding Y, French B, Tseng GC, Sibille E. Beyond modules and hubs: the potential of gene coexpression networks for investigating molecular mechanisms of complex brain disorders. *Genes Brain Behav*. 2014;13:13–24.
- Eisen MB, Spellman PT, Brown PO, Botstein D. Cluster analysis and display of genome-wide expression patterns. *Proc Natl Acad Sci USA*. 1998;95:14863–8.
- Fromer M, Roussos P, Sieberts SK, Johnson JS, Kavanagh DH, Perumal TM, et al. Gene expression elucidates functional impact of polygenic risk for schizophrenia. *Nat Neurosci*. 2016;19:1442–53.
- Gao X, Sakai K, Roberts RC, Conley RR, Dean B, Tamminga CA. Ionotropic glutamate receptors and expression of N-Methyl-D-aspartate receptor subunits in subregions of human hippocampus: effects of schizophrenia. *Am J Psychiatry*. 2000;157:1141–9.
- Kolomeets NS, Orlovskaya DD, Rachmanova VI, Uranova NA. Ultrastructural alterations in hippocampal mossy fiber synapses in schizophrenia: a postmortem morphometric study. *Synapse*. 2005;57:47–55.
- Schizophrenia Working Group of the Psychiatric Genomics C. Biological insights from 108 schizophrenia-associated genetic loci. *Nature*. 2014;511:421–7.

35. Mexal S, Berger R, Logel J, Ross RG, Freedman R, Leonard S. Differential regulation of $\alpha 7$ nicotinic receptor gene (CHRNA7) expression in schizophrenic smokers. *J Mol Neurosci*. 2010;40:185–95.
36. Gouvêa ES, Santos Filho AF, Ota VK, Mrad V, Gadelha A, Bressan RA, et al. The role of the CNR1 gene in schizophrenia: a systematic review including unpublished data. *Rev Bras Psiquiatr*. 2017;39:160–71.
37. Kang WS, Park JK, Kim SK, Park HJ, Lee SM, Song JY, et al. Genetic variants of GRIA1 are associated with susceptibility to schizophrenia in Korean population. *Mol Biol Rep*. 2012;39:10697–703.
38. Fang J, Wang Y, Lv X, Shen X, Ni X, Ding K. Structure of a β -glucan from *Grifola frondosa* and its antitumor effect by activating Dectin-1/Syk/NF- κ B signaling. *Glycoconj J*. 2012;29:365–77.
39. Fric J, Zelante T, Wong AYW, Mertes A, Yu H-B, Ricciardi-Castagnoli P, et al. NFAT control of innate immunity. *Blood*. 2012;120:1380–9.
40. Sancho D, Reis e Sousa C. Signaling by myeloid C-type lectin receptors in immunity and homeostasis. *Annu Rev Immunol*. 2012;30:491–529.
41. Plato A, Willment JA, Brown GD. C-type lectin-like receptors of the dectin-1 cluster: ligands and signaling pathways. *Int Rev Immunol*. 2013;32:134–56.
42. Iwakura Y, Nawa H. ErbB1-4-dependent EGF/neuregulin signals and their cross talk in the central nervous system: pathological implications in schizophrenia and Parkinson's disease. *Front Cell Neurosci*. 2013;7:1–13.
43. Potvin S, Stip E, Sepehry AA, Gendron A, Bah R, Kouassi E. Inflammatory cytokine alterations in schizophrenia: a systematic quantitative review. *Biol Psychiatry*. 2008;63:801–8.
44. Fillman SG, Cloonan N, Catts VS, Miller LC, Wong J, McCrossin T, et al. Increased inflammatory markers identified in the dorso-lateral prefrontal cortex of individuals with schizophrenia. *Mol Psychiatry*. 2013;18:206–14.
45. Pasternak O, Kubicki M, Shenton ME. In vivo imaging of neuroinflammation in schizophrenia. *Schizophr Res*. 2016;173:200–12.
46. Trépanier MO, Hopperton KE, Mizrahi R, Mechawar N, Bazinet RP. Postmortem evidence of cerebral inflammation in schizophrenia: a systematic review. *Mol Psychiatry*. 2016;21:1009–26.
47. van Kesteren CF, Gremmels H, de Witte LD, Hol EM, Van Gool AR, Falkai PG, et al. Immune involvement in the pathogenesis of schizophrenia: a meta-analysis on postmortem brain studies. *Transl Psychiatry*. 2017;7:1–11.
48. Hwang Y, Kim J, Shin JY, Kim JII, Seo JS, Webster MJ, et al. Gene expression profiling by mRNA sequencing reveals increased expression of immune/inflammation-related genes in the hippocampus of individuals with schizophrenia. *Transl Psychiatry*. 2013;3:1–9.
49. Crespo-Facorro B, Prieto C, Sainz J. Schizophrenia gene expression profile reverted to normal levels by antipsychotics. *Int J Neuropsychopharmacol*. 2015;18:1–7.
50. Santoro ML, Ota VK, Stilhano RS, Silva PN, Santos CM, Diana MC, et al. Effect of antipsychotic drugs on gene expression in the prefrontal cortex and nucleus accumbens in the spontaneously hypertensive rat (SHR). *Schizophr Res*. 2014;157:163–8.
51. Kalmady SV, Agrawal R, Venugopal D, Shivakumar V, Amaresha AC, Agarwal SM, et al. CHRFA7A gene expression in schizophrenia: clinical correlates and the effect of antipsychotic treatment. *J Neural Transm*. 2018;125:741–8.
52. Kaplan MS, Hinds JW. Neurogenesis in the adult rat: electron microscopic analysis of light radioautographs. *Science*. 1977;197:1092–4.
53. Maekawa M, Takashima N, Arai Y, Nomura T, Inokuchi K, Yuasi S, et al. Pax6 is required for production and maintenance of progenitor cells in postnatal hippocampal neurogenesis. *Genes Cells*. 2005;10:1001–14.
54. Sakurai K, Osumi N. The neurogenesis-controlling factor, pax6, inhibits proliferation and promotes maturation in murine astrocytes. *J Neurosci*. 2008;28:4604–12.
55. Klempin F, Marr RA, Peterson DA. Modification of Pax6 and Olig2 expression in adult hippocampal neurogenesis selectively induces stem cell fate and alters both neuronal and glial populations. *Stem Cells*. 2012;30:500–9.
56. Dwyer DS, Weeks K, Aamodt EJ. Drug discovery based on genetic and metabolic findings in schizophrenia. *Expert Rev Clin Pharmacol*. 2008;1:773–89.
57. Weeks KR, Dwyer DS, Aamodt EJ. Antipsychotic drugs activate the *C. elegans* AKT pathway via the DAF-2 insulin/IGF-1 receptor. *ACS Chem Neurosci*. 2010;1:463–73.
58. Bowling H, Zhang G, Bhattacharya A, Pérez-Cuesta LM, Deinhardt K, Hoeffler CA, et al. Antipsychotics activate mTORC1-dependent translation to enhance neuronal morphological complexity. *Sci Signal*. 2014;7:4.
59. Mchugh TJ, Jones MW, Quinn JJ, Balthasar N, Coppari R, Elmquist JK, et al. Dentate Gyrus NMDA receptors mediate rapid pattern separation in the hippocampal network. *Science*. 2007;317:94–99.
60. Tronel S, Belnoue L, Grosjean N, Revest JM, Piazza PV, Koehl M, et al. Adult-born neurons are necessary for extended contextual discrimination. *Hippocampus*. 2012;22:292–8.
61. Clelland CD, Choi M, Romberg C, Clemenson GD, Fagniere A, Tyers P, et al. A functional role for adult hippocampal neurogenesis in spatial pattern separation. *Science*. 2009;325:210–3.
62. Sommer IE, de Witte L, Begemann M, Kahn RS. Nonsteroidal anti-inflammatory drugs in schizophrenia. *J Clin Psychiatry*. 2012;73:414–9.
63. Nitta M, Kishimoto T, Müller N, Weiser M, Davidson M, Kane JM, et al. Adjunctive use of nonsteroidal anti-inflammatory drugs for schizophrenia: a meta-analytic investigation of randomized controlled trials. *Schizophr Bull*. 2013;39:1230–41.
64. Konstantinopoulos PA, Lehmann DF. The cardiovascular toxicity of selective and nonselective cyclooxygenase inhibitors: Comparisons, contrasts, and aspirin confounding. *J Clin Pharmacol*. 2005;45:742–50.
65. Lyketsos CG, Breitner JCS, Green RC, Martin BK, Meinert C, Piantadosi S, et al. Naproxen and celecoxib do not prevent AD in early results from a randomized controlled trial. *Neurology*. 2007;68:1800–8.
66. Martin BK, Szekely C, Brandt J, Piantadosi S, Breitner JCS, Craft S, et al. Cognitive function over time in the Alzheimer's disease anti-inflammatory prevention trial (ADAPT): Results of a randomized, controlled trial of naproxen and celecoxib. *Arch Neurol*. 2008;65:896–905.
67. Cimino PJ, Sokal I, Leverenz J, Fukui Y, Montine TJ. DOCK2 is a microglial specific regulator of central nervous system innate immunity found in normal and Alzheimer's disease brain. *Am J Pathol*. 2009;175:1622–30.
68. Dissing-Olesen L, LeDue JM, Rungta RL, Hefendehl JK, Choi HB, MacVicar BA. Activation of neuronal NMDA receptors triggers transient ATP-mediated microglial process outgrowth. *J Neurosci*. 2014;34:10511–27.
69. Eyo UB, Peng J, Swiatkowski P, Mukherjee A, Bispo A, Wu LJ. Neuronal hyperactivity recruits microglial processes via neuronal NMDA receptors and microglial P2Y12 receptors after status epilepticus. *J Neurosci*. 2014;34:10528–40.
70. Wu Y, Dissing-Olesen L, MacVicar BA, Stevens B. Microglia: dynamic mediators of synapse development and plasticity. *Trends Immunol*. 2015;36:605–13.
71. Parkhurst CN, Yang G, Ninan I, Savas JN, Yates JR, Lafaille JJ, et al. Microglia promote learning-dependent synapse formation through brain-derived neurotrophic factor. *Cell*. 2013;155:1596–609.

72. Yao I, Iida J, Nishimura W, Hata Y. Synaptic localization of SAPAP1, a synaptic membrane-associated protein. *Genes Cells*. 2003;8:121–9.
73. Shin SM, Zhang N, Hansen J, Gerges NZ, Pak DT, Sheng M, et al. GKAP orchestrates activity-dependent postsynaptic protein remodeling and homeostatic scaling. *Nat Neurosci*. 2012;15:1655–66.
74. Kohen R, Dobra A, Tracy JH, Haugen E. Transcriptome profiling of human hippocampus dentate gyrus granule cells in mental illness. *Transl Psychiatry*. 2014;4:e366.
75. Collado-Torres L, Burke EE, Peterson A, Shin JH, Straub RE, Rajpurohit A, et al. Regional heterogeneity in gene expression, regulation, and coherence in the frontal cortex and hippocampus across development and schizophrenia. *Neuron*. 2019;103:203–e8.
76. Bobilev AM, Perez JM, Tamminga CA. Molecular alterations in the medial temporal lobe in schizophrenia. *Schizophr Res*. 2019. <https://doi.org/10.1016/j.schres.2019.06.001>.